ISBN: 978-3-95450-227-1 ISSN: 2673-5490 doi:10.18429/JACoW-IPAC2022-TUPOMS041

HIGH POWER RF-CAVITY DEVELOPMENT FOR THE HBS-DRIVER LINAC

M. Basten * [1,2], K. Aulenbacher [1,2,3], W. Barth[1,2,3], C. Burandt[1,2], F. Dziuba[1,2,3], V. Gettmann[1,2], T. Gutberlet[4], T. Kürzeder[1,2], S. Lauber [1,2,3], J. List[1,2,3], M. Miski-Oglu[1,2], H. Podlech[5,6], M. Vossberg[1], S. Yaramyshev[1,2]

[1] GSI Helmholtzzentrum für Schwerionenforschung GmbH, Darmstadt, Germany
[2] HIM Helmholtz Institute Mainz, Mainz, Germany
[3] KPH Johannes Gutenberg-University Mainz, Mainz, Germany
[4] JCNS Forschungszentrum Jülich GmbH, Jülich, Germany
[5] IAP Institut für Angewandte Physik, Frankfurt am Main, Germany
[6] Helmholtz Research Academy Hesse for FAIR HFHF, Frankfurt am Main, Germany

Abstract

Neutron research in Europe is mainly based on various nuclear reactors that will be successively decommissioned over the next years. This means that despite the commissioning of the European Spallation Source ESS, many neutron research centres, especially in the medium flux regime, will disappear. In response to this situation, the Jülich Centre for Neutron Science (JCNS) has begun the development of a scalable, compact, accelerator-based High Brilliance neutron Source (HBS). A total of three different neutron target stations are planned, which can be operated with a 100 mA proton beam of up to 70 MeV and a duty cycle of up to 6 %. The driver Linac consists of an Electron Cyclotron Resonance (ECR) ion source followed by a LEBT section, a 2.5 MeV double Radio-Frequency Quadrupole (RFQ) and 35 normal conducting (NC) Crossbar H-Mode (CH) cavities. The development of the cavities is carried out by the Institute for Applied Physics (IAP) at the Goethe University Frankfurt am Main. Due to the high beam current, all cavities as well as the associated tuners and couplers have to be optimised for operation under high thermal load to ensure safe operation. In collaboration with the GSI Centre for Heavy Ion Research as the ideal test facility for high power tests, two cavities and the associated hardware are being designed and will be tested. The design and latest status of both cavities will be presented in this paper.

INTRODUCTION

RF cavities that are operated with high duty cycles or with high beam currents must, on the one hand, have an efficient cooling concept that limits the maximum temperature within the cavities. On the other hand, corresponding tuners must be able to compensate for the frequency change caused by the heating of the cavity and the RF power couplers must be optimised accordingly to ensure stable long-term operation. The GSI Centre for Heavy Ion Research has a long history of developing and operating various types of RF resonators, making it an ideal test facility for both cavities and the associated infrastructure. In collaboration with JCNS and with strong support by the HBS Innovationspool Project, two NC cavities together with the associated tuners and power couplers have been optimised for operation in continuous wave (CW) mode. These cavities will be used as prototypes for the HBS project [1–3] as well as for a new CW operated HElmholtz LInear ACcelerator (HELIAC) [4–8] which is currently under development at GSI and Helmholtz-Institute Mainz (HIM) [9, 10]. HELIAC will continue to enable experiments with long pulses and high repetition rates previously provided by the UNIversal Linear ACcelerator (UNILAC), which will in future provide high-intensity short-pulse beams for the Facility for Antiproton and Ion Research (FAIR) [11–18]. The HELIAC itself comprises a NC injector based on an ECR ion source, an RFQ and two Interdigital H-Mode (IH) cavities [19] followed by four cryomodules with superconducting (SC) CH-type cavities [5, 20, 21]. Together, they allow for an acceleration of heavy ions ($A/Z \leq 6$) to variable output energies ranging from 3.5 MeV/u to 7.3 MeV/u, with an energy spread less than ±3 keV/u. The overall parameters of the HELIAC are shown in Table 1.

Table 1: Design Parameters of the HELIAC

Mass/charge	≤6
Max. beam current	1 mA
Repetition rate	continuous wave
Output energy	3.5 – 7.3 MeV/u
Output energy spread	±3 keV/u
Frequency NC injector	108.408 MHz
Frequency SC accelerator	216.816 MHz

Both NC injector DTL cavities are based on the concept of Alternating Phase Focusing (APF), which applies synchronous phase changes between negative and positive phases to provide for successive transversal and longitudinal focusing during the acceleration [22]. This allows long accelerating sections with full transmission without the need for additional magnetic focusing elements.

* m.basten@gsi.de

ISBN: 978-3-95450-227-1 ISSN: 2673-5490 doi:10.18429/JACoW-IPAC2022-TUPOMS041

CAVITY LAYOUT

Two IH-type cavities of the HELIAC injector based on an APF beam dynamics concept were designed and optimised to serve as test cavities for the HBS project. Each cavity consists of a middle frame covered by two half-shells, as shown in Fig. 1. Since the stems and drift tubes are fixed on top of the girders with screws and nuts in the specified position, they can only be cooled indirectly via the girders. To ensure a most efficient cooling of the girders it is crucial that the cooling channel inside each girder is as close to the surface as possible. For this reason, the middle frame is milled together with the two girders as one component from a block of forged mild steel, which has a higher thermal conductivity than stainless steel.

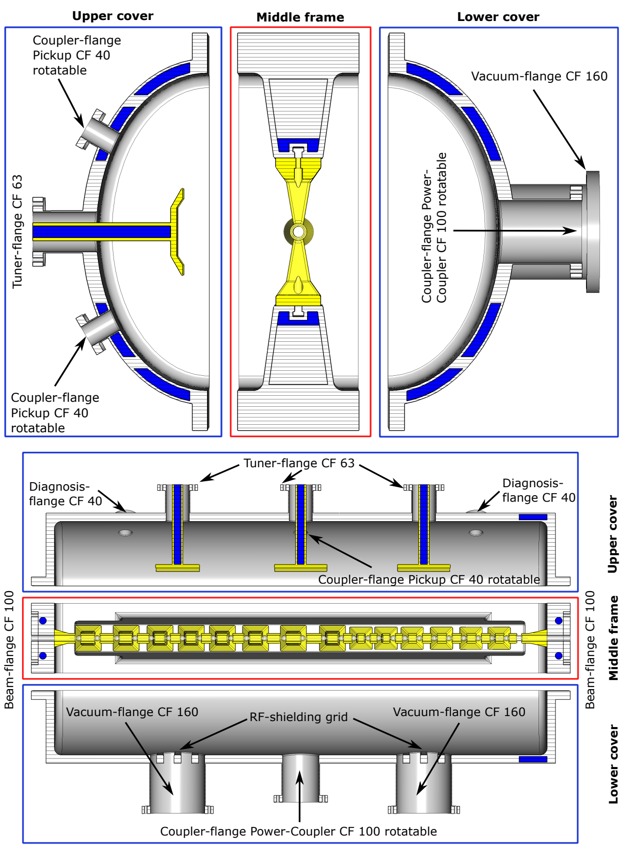

Figure 1: Transversal (top) and longitudinal (bottom) cross-section through the technical construction of the APF-IH cavities, consisting of a middle frame and two cavity half-shells, as well as three tuners for frequency adjustments.

MULTI-PHYSICS SIMULATIONS

To determine critical parameters like the maximum temperature and the resulting frequency shift due to the mechanical deformation of each cavity, we used CST Microwave Studio [23]. The electromagnetic fields and power loss distribution simulated with the eigenmode solver were used as input for the thermal solver to determine the temperature distribution in each cavity. This temperature distribution was then used as input for the mechanical solver to determine the deformation of each cavity. Finally, these results were used in the eigenmode solver to determine the frequency shift resulting from the mechanical deformation due to the temperature distribution.

By default, the thermal solver of CST assumes ideal thermal contact between contacting components and thus represents an optimistic estimate. In order to obtain on the one hand a realistic and on the other hand a pessimistic estimate of the temperature distribution in each cavity, a thermal resistance was defined at all crucial transitions, limiting the heat transfer between the individual components. For the pessimistic estimate, a thermal resistance of 1×10^{-3} K m^2/W was used between the girders and the stems as well as between the cooling water and the surrounding material. This thermal resistance corresponds to an air gap of approx. 26 µm and refers to the data from comparable applications at the Compact Intense Fast NEutron Facility CIFNEF [24, 25]. Since the worst thermal contact will be between the stems and the girders, a reduced thermal resistance of 1×10^{-4} K m^2/W was applied to the cooling water, while the full thermal resistance of 1×10^{-3} K m^2/W was kept between the girders and the stems to get a realistic estimate of the temperature distribution in each cavity.

Table 2: Maximum simulated temperature of APF-IH 1 and APF-IH 2 for the optimistic, pessimistic and realistic simulations

Max. simulated Temperature / K	APF-IH 1	APF-IH 2
Optimistic	350	360
Pessimistic	429	487
Realistic	413	441

The thermal resistance surrounding the cooling water compensates for the fact that the cooling water was kept at room temperature in all simulations and neither the cooling water flow nor the increase in cooling water temperature were taken into account. The results of APF-IH 1 and APF-IH 2 for all three cases are shown in Table 2 while the temperature distribution for the realistic case is shown in Fig. 2.

Table 3: Maximum simulated deformation of APF-IH 1 and APF-IH 2 caused by the optimistic, pessimistic and realistic temperature distribution

Max. simulated Deformation / mm	APF-IH 1	APF-IH 2
Optimistic	0.19	0.45
Pessimistic	0.43	1.03
Realistic	0.30	0.59

In the next step, the different temperature distributions were used to simulate the resulting mechanical deformation. Due to the temperature gradient along the individual stems and the large surface area of the two half-shells, the strongest deformations occur in the middle of the half-shells and along

ISBN: 978-3-95450-227-1 ISSN: 2673-5490 doi:10.18429/JACoW-IPAC2022-TUPOMS041

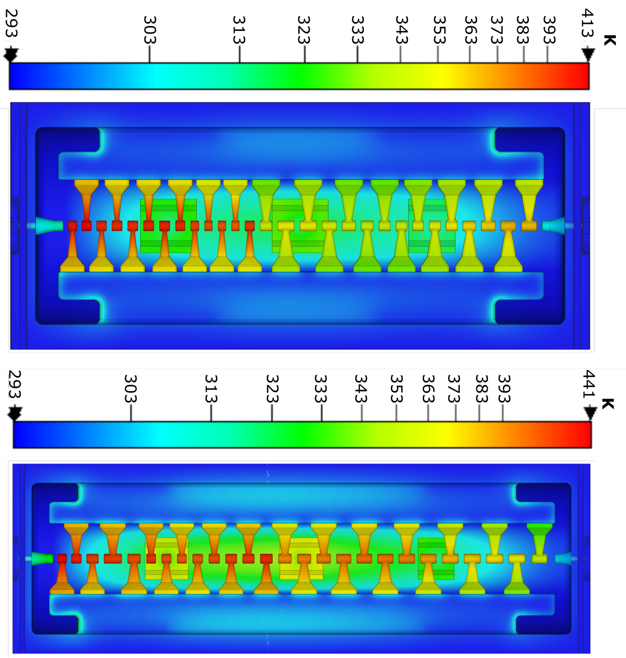

Figure 2: Temperature distribution of APF-IH 1 (top) and APF-IH 2 (bottom) for the realistic case with thermal resistance of 1×10^{-3} K m^2/W between stems and girder and 1×10^{-4} K m^2/W between cooling water and surrounding metal at their design gradient. Simulated with CST.

the stems. The expansion of the individual stems causes the drift tubes to move against each other away from the beam axis, while the half-shells are pushed apart. The maximum simulated deformation of APF-IH 1 and APF-IH 2 for the different temperature distributions is shown in Table 3.

Table 4: Simulated frequency change of APF-IH 1 and APF-IH 2 due to the deformations caused by the optimistic, pessimistic and realistic temperature distributions

Frequency change / kHz	APF-IH 1	APF-IH 2
Optimistic	-139	-241
Pessimistic	-460	-821
Realistic	-334	-547

In the final step, the simulated mechanical deformation of each cavity was used to determine the resulting frequency shift using CST's eigenmode solver. The simulated frequency change in each cavity for the optimistic, pessimistic and realistic temperature distribution is shown in Table 4.

TUNING CONCEPT

It is crucial that both cavities can be operated at the desired target frequency with different RF loads. Therefore, each cavity is equipped with three tuners to compensate for the expected frequency change shown in Table 4. For the realistic estimation, we expect a frequency change of no more than −330 kHz for APF-IH 1 and −550 kHz for APF-IH 2. The combined tuning range of all three tuners is between +330 kHz and -825 kHz for APF-IH 1 and between +450 kHz and -640 kHz for APF-IH 2, as shown in Fig. 3. This is just sufficient for APF-IH 1 but not enough to compensate the expected −550 kHz of APF-IH 2. For this reason the nominal tuner height of APF-IH 2 will be increased to extend the tuning range towards positive frequency deviations. The final layout and parameters of both cavities can be found in [19].

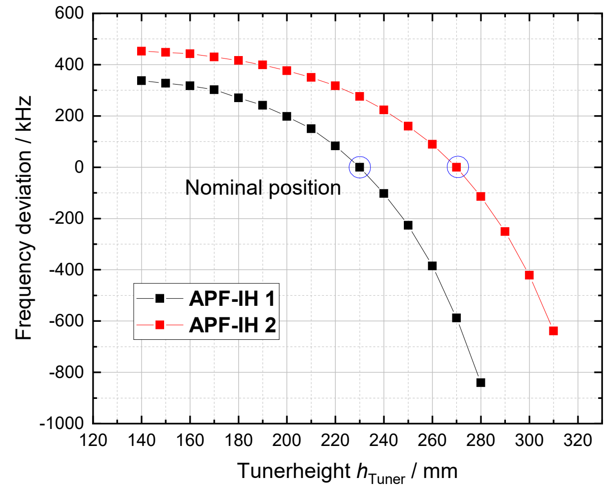

Figure 3: Combined tuning range of all tuners for APF-IH 1 and APF-IH 2 with nominal tuner position at h_{Tuner} = 230 mm for APF-IH 1 and h_{Tuner} = 270 mm for APF-IH 2.

CONCLUSION

Two IH cavities based on an APF beam dynamics scheme have been designed and optimised for CW operation in an heavy ion linear accelerator. Both cavities also serve as prototypes for the upcoming HBS project in order to test long-term operation at high power levels. Detailed Multi-Physics simulations have been performed to determine and optimise the temperature distribution in both cavities and evaluate the mechanical deformation and resulting resonance frequency change. This frequency change can be compensated for by the combined tuning range of three tuners in each cavity, which keep the cavities at the design resonance frequency at different duty cycles. The presented cavities are thermally and mechanically suitable for CW operation with a cooling concept that allows a comparatively low temperature increase at high RF power levels. Both cavities are currently in production and will be delivered in summer 2023 to be copper-plated and tested at full RF power.

ACKNOWLEDGEMENTS

The authors would like to thank the HBS Innovationspool Project for the strong support of the presented work, both financially and in practical terms.

ISBN: 978-3-95450-227-1 ISSN: 2673-5490 doi:10.18429/JACoW-IPAC2022-TUPOMS041

REFERENCES

[1] U. Rücker *et al.*, "The Jülich high brilliance neutron source project," *Eur. Phys. J. Plus, vol. 131, no. 19*, 2016, doi:10.1140/epjp/i2016-16019-5

[2] T. Gutberlet *et al.*, "The Jülich high brilliance neutron source project - Improving access to neutrons," *Physica B: Condensed Matter*, 2019, doi:10.1016/j.physb.2018.01.019

[3] H. Podlech *et al.*, "Conceptual Design of the Proton LINAC for the High Brilliance Neutron Source HBS," in *Proc. IPAC'19*, 2019, pp. 910–913, doi:10.18429/JACoW-IPAC2019-MOPTS027

[4] S. Minaev, U. Ratzinger, H. Podlech, M. Busch, and W. Barth, "Superconducting, energy variable heavy ion linac with constant β, multicell cavities of CH-type," *Phys. Rev. ST Accel. Beams*, vol. 12, p. 120 101, 2009, doi:10.1103/PhysRevSTAB.12.120101

[5] M. Schwarz, S. Yaramyshev, K. Aulenbacher, W. Barth, M. Basten, *et al.*, "Reference beam dynamics layout for the SC CW heavy ion HELIAC at GSI," *Nucl. Instr. Meth. Phys. Res. Sect. A*, p. 163 044, 2019, doi:10.1016/j.nima.2019.163044

[6] W. Barth, K. Aulenbacher, M. Basten, M. Busch, F. Dziuba, *et al.*, "First heavy ion beam tests with a superconducting multigap CH cavity," *Phys. Rev. Accel. Beams*, vol. 21, p. 020 102, 2018, doi:10.1103/PhysRevAccelBeams.21.020102

[7] W. Barth, K. Aulenbacher, M. Basten, F. Dziuba, V. Gettmann, *et al.*, "A superconducting CW-linac for heavy ion acceleration at GSIX," *EPJ Web Conf.*, vol. 138, p. 01 026, 2017, doi:10.1051/epjconf/201713801026

[8] S. Lauber, K. Aulenbacher, W. Barth, M. Basten, C. Burandt, *et al.*, "A dynamic collimation and alignment system for the helmholtz linear accelerator," *Review of Scientific Instruments*, vol. 92, no. 11, p. 113 306, 2021, doi:10.1063/5.0069824

[9] W. Barth, K. Aulenbacher, M. Basten, M. Busch, F. Dziuba, *et al.*, "Superconducting CH-cavity heavy ion beam testing at GSI," *J. Phys. Conf. Ser.*, vol. 1067, p. 052 007, 2018, doi:10.1088/1742-6596/1067/5/052007

[10] F. Dziuba, K. Aulenbacher, W. Barth, M. Basten, C. Burandt, *et al.*, "Further RF measurements on the superconducting 217 MHz CH demonstrator cavity for a CW linac at GSI," *J. Phys. Conf. Ser.*, vol. 1350, p. 012 185, 2019, doi:10.1088/1742-6596/1350/1/012185

[11] W. Barth, U. Scheeler, H. Vormann, M. Miski-Oglu, M. Vossberg, S. Yaramyshev, *et al.*, "High brilliance beam investigations at the universal linear accelerator," *Phys. Rev. ST Accel. Beams*, vol. 25, p. 040 101, 2022, doi:10.1103/PhysRevAccelBeams.25.040101

[12] W. Barth, W. Bayer, L. Dahl, L. Groening, S. Richter, *et al.*, "Upgrade program of the high current heavy ion UNILAC as an injector for FAIR," *Nucl. Instr. Meth. Phys. Res. Sect. A*, vol. 577, no. 1, pp. 211–214, 2007, doi:10.1016/j.nima.2007.02.054

[13] W. Barth, A. Adonin, C. Düllmann, M. Heilmann, R. Hollinger, *et al.*, "High brilliance Uranium beams for the GSI FAIR," *Phys. Rev. ST Accel. Beams*, vol. 20, p. 050 101, 2017, doi:10.1103/PhysRevAccelBeams.20.050101

[14] W. Barth, A. Adonin, C. E. Düllmann, M. Heilmann, R. Hollinger, *et al.*, "U^{28+}-intensity record applying a H_2-gas stripper cell," *Phys. Rev. ST Accel. Beams*, vol. 18, p. 040 101, 4 2015, doi:10.1103/PhysRevSTAB.18.040101

[15] A. Adonin and R. Hollinger, "Beam brilliance investigation of high current ion beams at GSI heavy ion accelerator facility," *Rev. Sci. Instrum.*, vol. 85, 02A727, 2014, doi:10.1063/1.4833931

[16] S. Yaramyshev, H. Vormann, A. Adonin, W. Barth, L. Dahl, *et al.*, "Virtual charge state separator as an advanced tool coupling measurements and simulations," *Phys. Rev. ST Accel. Beams*, vol. 18, 2015, doi:10.1103/PhysRevSTAB.18.050103

[17] W. Barth, A. Adonin, S. Appel, P. Gerhard, M. Heilmann, *et al.*, "Heavy ion linac as a high current proton beam injector," *Phys. Rev. ST Accel. Beams*, vol. 18, p. 050 102, 2015, doi:10.1103/PhysRevSTAB.18.050102

[18] A. Adonin, W. Barth, F. Heymach, R. Hollinger, H. Vormann, *et al.*, "Production of high current proton beams using complex H-rich molecules at GSI," *Rev. Sci. Instrum.*, vol. 87, 02B709, 2016, doi:10.1063/1.4934620

[19] M. Basten *et al.*, "Continuous Wave Interdigital H-Mode Cavities for Alternating Phase Focusing Heavy Ion Acceleration," (submitted to RSI).

[20] H. Podlech, U. Ratzinger, H. Klein, C. Commenda, H. Liebermann, *et al.*, "Superconducting CH structure," *Phys. Rev. ST Accel. Beams*, vol. 10, 2007, doi:10.1103/PhysRevSTAB.10.080101

[21] F. Dziuba, M. Busch, M. Amberg, H. Podlech, C. Zhang, *et al.*, "Development of superconducting crossbar-H-mode cavities for proton and ion accelerators," *Phys. Rev. ST Accel. Beams*, vol. 13, no. 4, 2010, doi:10.1103/PhysRevSTAB.13.041302

[22] S. Lauber *et al.*, "An alternating phase focusing injector or heavy ion acceleration," (submitted to NIMA).

[23] *CST MicroWave Studio*, www.cst.com, Accessed: 2021-07-21, www.cst.com

[24] H. Li, Z. Wang, Q. Lu Y.R.and Tan, M. Easton, K. Zhu, *et al.*, "Design of a CW linac for the compact intense fast neutron facility," *Nucl. Instrum. Meth. Phys. Res. Sect. A*, vol. 930, pp. 156–166, 2019, doi:10.1016/j.nima.2019.03.086

[25] Q. Tan, M. Easton, Q. Fu, P. Gan, H. Li, *et al.*, "Multiphysics analysis of a CW IH-DTL for CIFNEF," in *Proc. IPAC'18*, Vancouver, BC, Canada, 2018, pp. 1129–1131, doi:10.18429/JACoW-IPAC2018-TUPAL052